Formation of segmented normal faults: a 3-D perspective

J.J. Walsh[a], W.R. Bailey[a,c], C. Childs[a,*], A. Nicol[b], C.G. Bonson[a]

[a]*Fault Analysis Group, Department of Geology, University College Dublin, Belfield, Dublin 4, Ireland*
[b]*Institute of Geological and Nuclear Sciences Ltd, PO Box 30 368, Lower Hutt, New Zealand*
[c]*CSIRO Petroleum, ARRC, 26 Dick Perry Ave, Kensington, WA 6151, Australia*

Abstract

The interpretation of fault kinematics from geometric data is an essential step in developing an understanding of the growth of fault systems. Constraints on fault geometry are, however, often restricted to 2-D maps or cross-sections. In this article we consider the extent to which kinematic interpretations of faulting benefit from a 3-D, rather than 2-D geometrical perspective. Concentrating on relay zones and segmented normal fault arrays, we suggest that very different interpretations of their evolution arise from the recognition that the propagation directions of faults, and fault segments, will rarely be contained within the inspection plane of 2-D data. A 3-D perspective favours an interpretation in which the segments of a fault array are kinematically interrelated from their initiation. Individual segments in such systems may link into a single fault surface out of the plane of inspection or may be unconnected in 3-D. We argue that this interpretation, which conflicts with the often suggested model of incidental overlap of originally isolated faults, should be the preferred model for the generation and growth of segmented normal fault arrays.
© 2002 Published by Elsevier Science Ltd.

Keywords: Segmented normal fault; Fault propagation; Fault growth

1. Introduction

Segmented fault arrays containing two or more fault segments (Fig. 1) are a common feature of faults on all scales (Walsh and Watterson, 1989, 1990, 1991; Peacock and Sanderson, 1991, 1994; Stewart and Hancock, 1991; Trudgill and Cartwright, 1994; Cartwright et al., 1995; Childs et al., 1995; Dawers and Anders, 1995; Huggins et al., 1995). Segmented arrays may show aggregate displacement variations that are similar to those of a single isolated fault (e.g. Walsh and Watterson, 1989, 1990; Peacock and Sanderson, 1991; Dawers and Anders, 1995) suggesting that they are elements of a single coherent structure. However, interpretations of the growth of segmented fault arrays most often involve early-stage nucleation and propagation of kinematically *independent* segments, followed by *incidental*[1] overlap, interaction and the formation of fault relay zones (Fig. 2a and b; e.g. Morley et al., 1990; Trudgill and Cartwright, 1994; Cartwright et al., 1995, 1996; Dawers and Anders, 1995; Contreras et al., 2000). This model requires that individual fault segments initially grew in isolation from other segments in the fault array and we refer to it as the 'isolated fault model'. The widespread endorsement of this model derives largely from the 2-D nature of most fault data. When interpreting fault trace data in either map or cross-section it is natural to invoke a 2-D growth model and assume that the propagation direction of each fault or fault segment is in the plane of inspection. Similarly, numerical models of fault system growth are usually 2-D (Cowie et al., 1993, 2000; Cowie, 1998; Gupta et al., 1998) so that fault propagation directions are constrained to the plane of the model; in such modelling schemes interaction between initially isolated segments is promoted. Although the isolated fault model can be expanded to 3-D it is based on 2-D observations, which are generally interpreted without considering that fault growth is a 3-D process.

Using 3-D constraints from seismic and outcrop data and acknowledging the importance of out-of-plane fault propagation, Childs et al. (1995, 1996b) suggest an alternative

[1] By *incidental* we mean that individual faults initiated as kinematically independent structures and began to interact by chance as defined by Huggins et al. (1995) and did *not* initiate as a coherent array as redefined by Mansfield and Cartwright (2001).
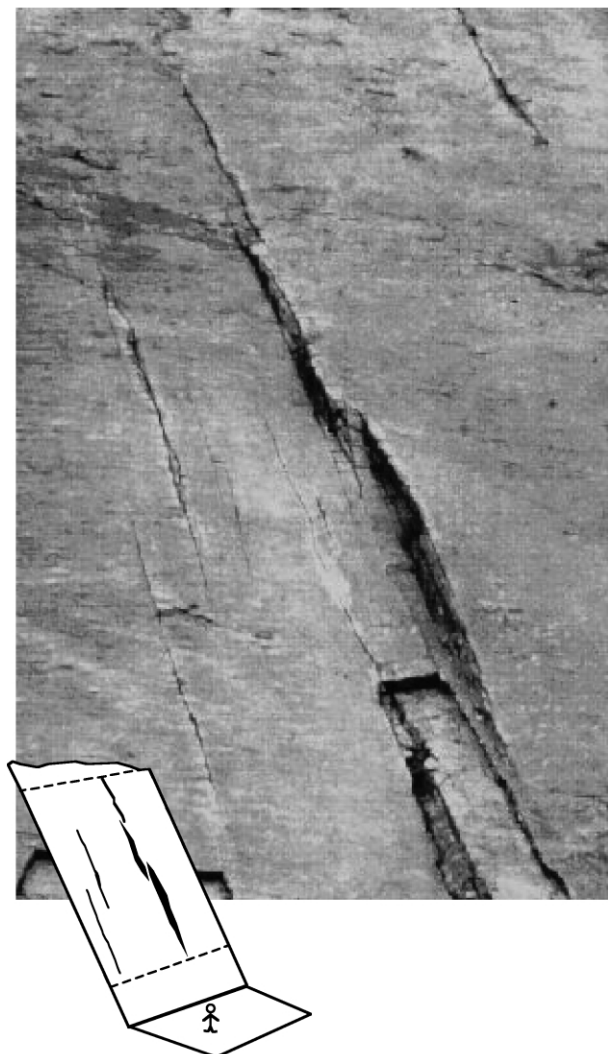
Fig. 1. Outcrop example of a fault array that comprises a number of segments separated by relay ramps. The view is of an inclined bedding surface (ca. 70°, see inset) displaced by a segmented strike-slip fault. The relationships between the bed and fault geometries at the segment boundaries are identical to those at a relay ramp between normal fault segments offsetting horizontal beds. The close spatial relationship between the segments and the sympathetic increases and decreases in displacement between adjacent segments, clearly indicates that these combine to form one structure. Sketch shows person for scale. Outcrop located at Jaca, Pyrenees, Spain.

model for the formation of segmented fault arrays, referred to hereafter as the 'coherent fault model'. In the coherent fault model individual fault segments initiate and grow as kinematically related components of a fault array. Fault segmentation may occur by fault surface bifurcation, i.e. splaying, resulting in fault segments that are hard-linked to a single fault out of the plane of inspection (Fig. 2c). Alternatively, fault segmentation may occur by stepping during propagation or localisation of an individual fault, giving rise to fault segments which are, at least initially, unconnected in three dimensions (Fig. 2d). These unconnected fault segments are soft-linked by ductile strain of the rock volume between them; to avoid confusion we refer to

this mode of segmentation as '3-D segmentation'. Relay zone formation in the coherent fault model is *not incidental* but is a product of bifurcation or 3-D segmentation processes. Although a comparable bifurcation model, based mainly on analysis of analogue models, is preferred for the formation of segmented strike-slip fault zones (Cloos, 1928; Riedel, 1929; Tchalenko, 1970; Richard et al., 1995), it is typically not favoured for normal faults.

The distinction between the two end-member models for the formation of segmented fault arrays is important, if conclusions are to be drawn regarding their growth and the growth of fault systems in general. Although both models are likely to be applicable in different circumstances, their relative importance has yet to be established. In our view the isolated fault model has achieved a degree of acceptance which is not merited by observation and this article attempts to redress this balance. In this paper we argue that the coherent fault model is the most parsimonious interpretation of the displacement distributions of most segmented fault arrays. We use new, as well as previously published, examples of segmented fault arrays together with analysis of an ideal elliptical fault model to outline evidence supporting the view that relay zones most often form with fault segments as components of a single kinematically coherent system.

2. Displacement distribution on segmented faults

The fundamental difference between the two models for formation of segmented fault arrays is the status of the individual fault segments when they initiate (Fig. 2). In the isolated fault model each segment initiates as a separate fault, which is spatially and mechanically unrelated to the array that it ultimately becomes a component of. In the coherent fault model each fault segment initiates as a component of a spatially and mechanically related array. The finite displacement distributions on segmented fault arrays that result from these two modes of formation will differ. Where fault segments were kinematically related from their initiation they will have complementary finite displacement distributions, which sum together to give a smooth and regular aggregate displacement distribution resembling that of a single isolated fault (Fig. 2e); pairs or groups of faults with such complementary displacements are referred to as geometrically coherent (Walsh and Watterson, 1991). In the isolated fault model the aggregate displacement distribution will have several local maxima, one located at the point of maximum displacement of each fault segment (Fig. 2b). Aggregate fault displacement distributions observed in 2-D or 3-D therefore provide the means for distinguishing between the basic end-member kinematic models for segmented faults (Fig. 2).

In general, aggregate displacements for segmented fault arrays display along-strike displacement variations that are often broadly comparable with those of individual isolated faults (Fig. 3; Walsh and Watterson, 1990; Peacock and
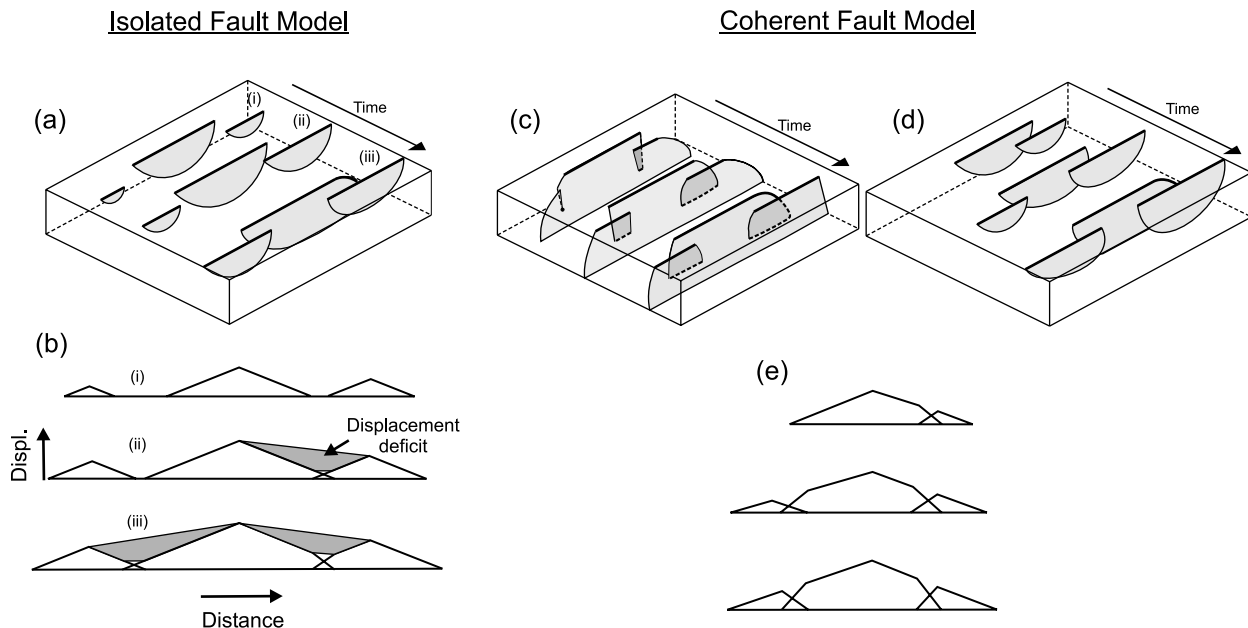
Fig. 2. Schematic illustrations of the two end-member models of formation of segmented fault arrays. The block diagrams (a, c and d) each show three stages in the growth of a segmented fault array (i–iii). The displacement-distance plots (b and e) are for the fault traces on the upper surfaces of the block diagrams (bold lines). The bold dashed lines in (c) indicate branch-lines. The coherent fault model is illustrated for segmented fault traces that are (c) hard-linked and formed by fault surface bifurcation and (d) soft-linked and formed by 3-D segmentation. The shaded areas in (b) indicate deficits in displacement between the adjacent fault segments, which are not due to continuous deformation within relay zones (see text). The aggregate displacement profiles (not shown) for the two models differ in that the points of maximum displacement are preserved where the faults were initially isolated (b–iii) but a simple aggregate profile occurs at all stages of development in the coherent fault model.

Sanderson, 1991; Dawers and Anders, 1995; Cartwright et al., 1996; Willemse, 1997). In detail these displacement variations are sometimes characterised by displacement lows at relay zones and between the centres of fault segments. In most of these cases, however, the displacement low is matched by an increase in fault-related folding and bed rotation that are often concentrated within relay zones (Fig. 4; Walsh and Watterson, 1990; Peacock and Sanderson, 1991; Childs et al., 1995; Dawers and Anders, 1995; Huggins et al., 1995). The inclusion of both the discontinuous (i.e. fault) and continuous (i.e. folds and bed rotations) displacements in estimates of the total, or aggregate, displacement across segmented faults is a crucial step in assessing whether an array is a geometrically coherent system (Peacock and Sanderson, 1994; Childs et al., 1995; Huggins et al., 1995; Walsh et al., 1996). When account is taken of both the discontinuous and continuous components of displacement and an aggregate displacement low still exists between the points of maximum displacement on adjacent segments (Fig. 2b), then it can be argued that individual segments were originally isolated faults that grew laterally, or vertically, to form a later, incidental relay zone. Few such displacement deficits are documented in the literature (but see Morley and Wonganan, 2000) and in their absence both of the alternative models for the formation of segmented normal fault systems have been advanced.

The coherent fault model directly accounts for the absence of a displacement deficit by considering that the formation of a relay zone is geologically instantaneous (i.e. formation is on

a timescale that is less than the temporal resolution of the growth data), and that the faults bounding the relay zone always formed a kinematically coherent system. By contrast, application of the isolated fault model to segment boundaries across which displacements are conserved has been attributed to the incidental overlap of faults with earlier deficits (Fig. 2b) removed by later preferential displacement at fault relay zones (Anders and Schlische, 1994; Dawers and Anders, 1995; Cartwright et al., 1996; Contreras et al., 2000; Gupta and Scholz, 2000). In the latter case the underlying assumption is that once initially isolated faults interact to form a segmented array, subsequent displacements accrue preferentially at the segment boundary to produce a displacement profile, and a displacement to length ratio, for the array which approaches that of a single fault. Such a scenario is only possible if initially isolated faults begin to interact early in their growth history. In these cases, while the faults were initially isolated, the segmented fault array would have developed in a kinematically coherent manner throughout much of its growth history making distinction between models problematic. This is partly because aggregate displacement deficits at the segment boundary produced prior to fault interaction will represent a small proportion of the total displacement and may be difficult to identify, particularly if measurement errors are significant (e.g. $> \pm 10$–20%). For those examples where fault segments are inferred to be isolated during much of their growth history a model in which post-interaction displacements are concentrated where original displacement deficits occurred
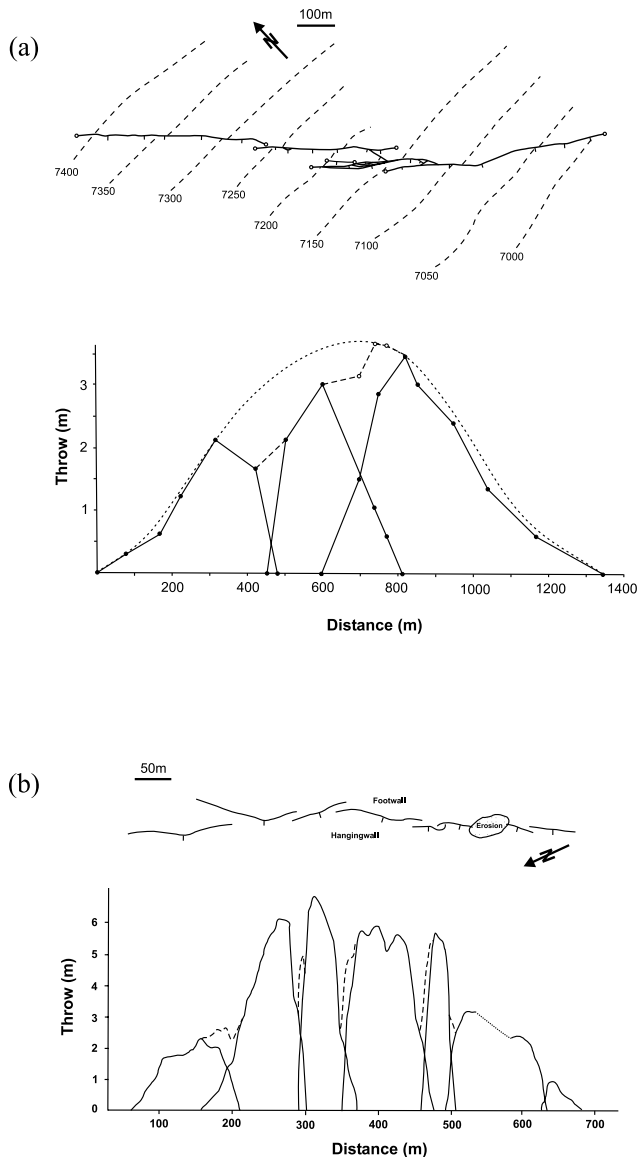
Fig. 3. (a) Map (top) and throw profiles (bottom) of a segmented normal fault recorded on Arley coal seam mine plans, Nook Colliery, Lancashire, UK (reproduced from Walsh and Watterson, 1990). The map shows coal seam height contours (dashed) and tip locations (open circles). The throw profile along the segmented fault array (solid lines) demonstrates that although the faults comprise three distinct segments, they behave as one kinematically coherent structure as highlighted by the idealised envelope plotted through the summed displacements (dashed line). (b) Segmented fault array in the Bishop Tuff, California showing a systematic distribution of throw along seven fault segments (solid lines). The aggregate throw profile is shown as dashed lines, but this does not include the strain accommodated by rotation of bedding with the relays zones. Reproduced from Willemse (1997).

(e.g. Contreras et al., 2000), can, in our view, only be justified if the displacement deficit is maintained by elastic deformation of the rock volume. Numerical models demonstrate the importance of elastic strains at relay zones in a single slip event (Willemse et al., 1996); however, large cumulative displacement deficits (e.g. decametre or greater), which accrue from numerous earthquake slip events over millions of
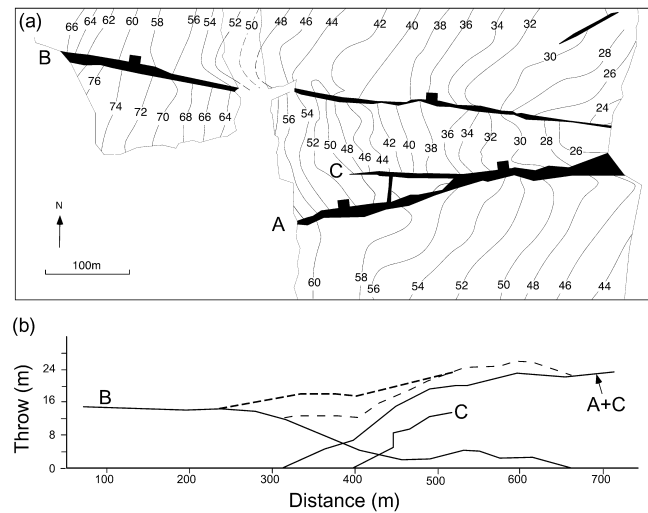

Fig. 4. Detailed structure of a relay ramp mapped on the Main coal seam in West Chevington East Extension open-cast site, Northumberland, UK. (a) Map of relay zone, showing seam elevation contours in metres. (b) Throw profiles along faults A, B and C. The aggregate fault throw profile (thin dashed line) and aggregate throw profile including continuous deformation within the ramp (heavy dashed line) are shown. These smooth aggregate throw profiles along the relay demonstrate that the array is essentially a single, coherent structure (reproduced from Huggins et al. (1995)).

years, cannot be sustained elastically and there is little reason for subsequent deformation to 'remember' that the deficits exist. We suggest that, at the very least, the absence of displacement deficits favours a model in which the fault segments formed a kinematically coherent system early in their growth history. In many cases, coherence may have been characteristic of segmented faults from their initiation with their development being a geologically instantaneous product of out-of-plane propagation.

3. Fault surface propagation

The isolated fault model of segmented fault formation is based mainly on 2-D data and the assumption that fault propagation occurs within that plane. Here we use a simple geometrical analysis to examine the likelihood that this assumption is true for an arbitrary 2-D section through a segmented fault array. Conceptual models of fault geometry are usually underpinned by the notion of a single isolated fault, in which displacement contours are approximately elliptical and decrease from a maximum close to the centre of the fault (Fig. 5; Watterson, 1986; Walsh and Watterson, 1987). Few faults strictly adhere to this simple model, but the vast majority can be considered variants on this basic theme, complicated by factors such as fault interaction, anisotropies that arise from the rheological differences between layers and from interaction with the free surface (Barnett et al., 1987; Childs et al., 1993, 2003; Nicol et al., 1996). Whatever the precise departure from this
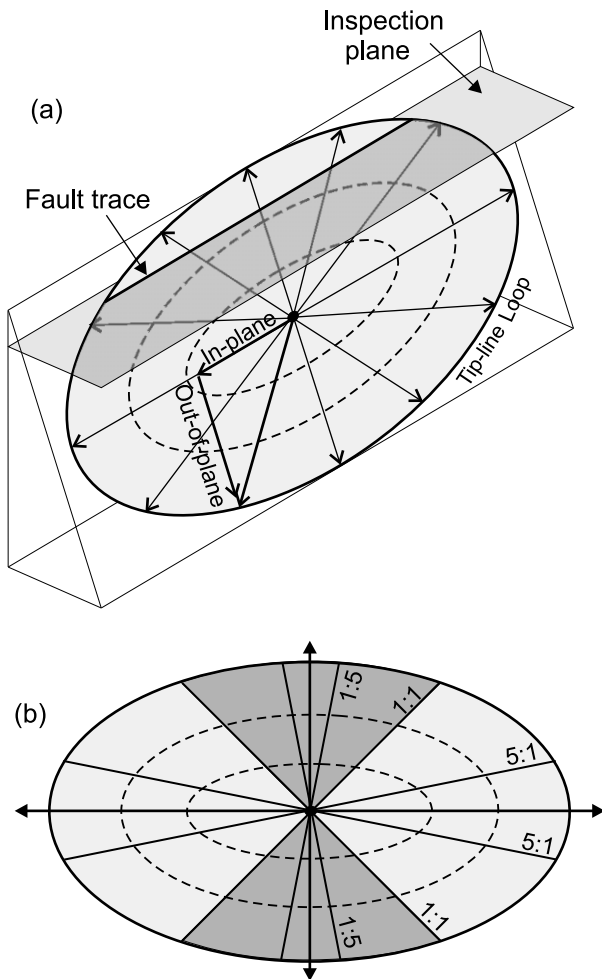
Fig. 5. (a) Schematic block diagram of an elliptical fault surface (aspect ratio 1.7) showing how radial propagation directions (arrows), and therefore components of in-plane and out-of-plane propagation, vary along a fault trace within a horizontal inspection plane. (b) Elliptical fault surface contoured according to the ratio of in-plane to out-of-plane propagation for horizontal planes of inspection. 1:1 lines divide parts of the fault surface dominated by vertical propagation (dark shading) and those dominated by horizontal propagation (light shading). Arrows show the positions of the principal axes of the ellipse along which there is solely horizontal or vertical propagation.

occur, which generally increases at lower angles between the plane and displacement contours. Therefore, 2-D samples of the fault surface that do not contain the maximum displacement are necessarily characterised by varying propagation directions along a fault trace. The significance of these changes is illustrated in Fig. 5b, which shows ratios of in-plane to out-of-plane propagation for horizontal planes of inspection on an elliptical fault surface. For this model only a small proportion (21%) of the fault surface is characterised by mainly, or entirely, in-plane propagation (e.g. ratios of 5:1 or greater, Fig. 5b).

Using ratios of in-plane to out-of-plane propagation (e.g. Fig. 5b) the proportion of a fault surface characterised by entirely in-plane propagation (e.g. ratios of 5:1 or greater) can be charted for different fault shapes. Fig. 6 was constructed by calculating the proportion of an elliptical fault surface with in-plane propagation (e.g. ratios of 5:1 or greater) for horizontal (map view) and vertical (cross-sections) inspection planes. This proportion increases as faults become more elongate parallel to the inspection plane. For a typical range of fault aspect ratios of between one and three we would expect in-plane propagation over up to 33% and 12% of the fault surface for horizontal and vertical planes of inspection, respectively. Therefore, for these fault aspect ratios, cross-sections are about one third less likely to exhibit entirely in-plane propagation than maps.

Despite the geometrical requirements to constrain 3-D propagation directions for an isolated fault, most previous studies of segmented normal faults use 2-D data and implicitly assume entirely within-plane fault propagation, even though faults may be sampled in cross-section (e.g.

simple model, an acceptance of 3-D propagation, which is ideally radial from the point of maximum displacement and at a high angle to displacement contours, is the paradigm (Fig. 5a). Recognition of the importance of 3-D fault propagation demands that a given inspection plane is unlikely to contain the propagation direction of a fault. For an ideal elliptical fault the propagation direction will be contained only within a plane that passes through the maximum displacement. In practice, as maps or cross-sections are most commonly used and because the principal axes of elliptical fault surfaces are typically horizontal and vertical, 2-D samples will exhibit exclusively in-plane propagation only when they contain a principal axis of the fault surface. For all other planar surfaces a component of out-of-plane propagation will
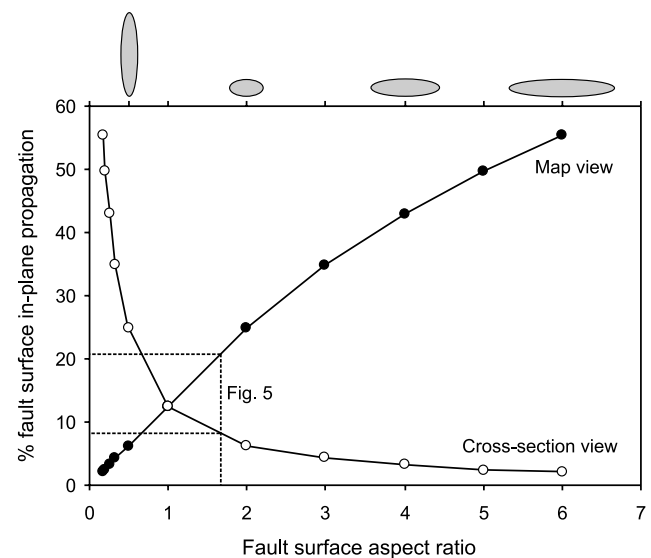

Fig. 6. Plot of % fault surface characterised by in-plane propagation (e.g. ratios of in-plane to out-of-plane propagation of 5:1 or greater) vs. fault surface aspect ratio for elliptical faults, which is also depicted along the top of the plot. The geometry of the fault ellipse presented in Fig. 5 is shown by the dashed lines.

Eisenstadt and De Paor, 1987; Mansfield and Cartwright, 1998; Marchal et al., 1998) or map view (Cartwright et al., 1995; Dawers and Anders, 1995; Contreras et al., 2000). Assumptions of within-plane propagation will only hold in these studies if the maximum displacement was fortuitously sampled or, in some cases, if fault surfaces are highly elongate parallel to the plane of inspection (Fig. 6). These conditions are unlikely to have been satisfied in the majority of cases as fault surfaces are rarely highly elongate (Rippon, 1985; Barnett et al., 1987; Chapman and Meneilly, 1991; Nicol et al., 1996), whilst the probability of sampling the maximum displacement in any given arbitrary plane will be low.

The analysis above refers to the ideal fault model for blind, isolated faults (see Watterson, 1986). In many cases, however, faults intersect the free surface during growth with fault movements and sedimentation or erosion occurring synchronously. In circumstances where it can be demonstrated that a fault intersected the free surface the plane of inspection is likely to be close to, or at, the free surface and the upper tip line of the fault. This plane is spatially removed from the maximum displacement and transects part of the fault surface dominated by displacement contours that are approximately horizontal (Barnett et al., 1987; Childs et al., 1993, 2003; Nicol et al., 1996). Therefore, growth faults form in association with a component of upward propagation near to the free surface and maps of these faults are likely to exhibit a significant component of out-of-plane propagation.

4. 3-D fault geometries

Interpretation of segmented fault arrays from map or cross-section data is further complicated by the recognition that individual fault segments on an arbitrary plane may link to form a single fault surface in the third dimension (Fig. 2c). The fault shown in Fig. 7 comprises two fault segments bounding a relay zone on a mapped horizon (Horizon A,
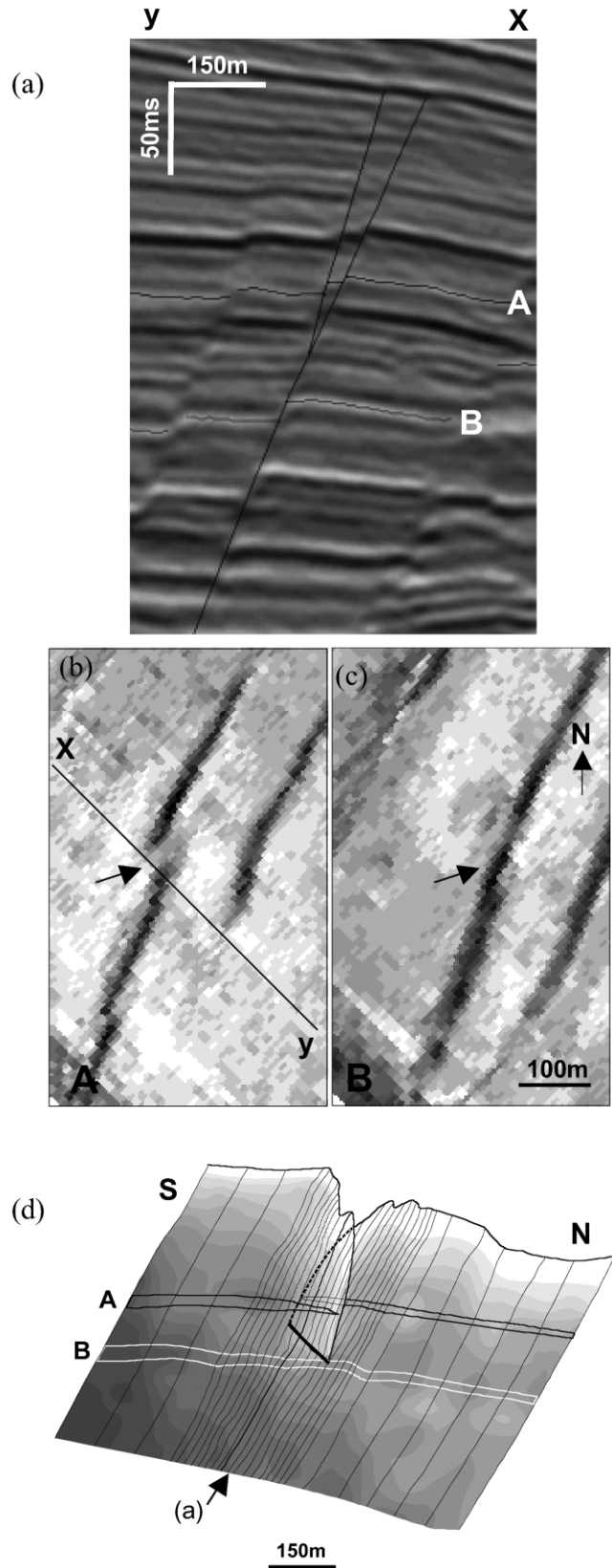

Fig. 7. Example of an upwardly bifurcating fault (max throw ~30 ms or 45 m) interpreted in a high resolution, 3-D seismic survey (line spacing 12.5 m; throw resolution down to 1 ms; 1 ms = ca 1.5 m). It is a synsedimentary fault that was active after deposition of Horizon A. The detailed structure of the relay zone has been interpreted on 18 seismic lines and displacements on the fault are mapped using six reflectors spaced over <200 ms vertical interval. (a) Seismic line showing cross-section of the upwardly branching geometry. (b and c) Coherence maps of reflectors A and B showing the change in structure with depth: arrow indicates the position of the relay zone. The dark areas highlight the faults. The location of the line of section in (a) is shown. (d) Three-dimensional oblique view of the fault, showing bifurcation upwards from a sub-horizontal branch-line (bold line). Shaded contours are for throw (dark grey shading at the bottom left of the fault plane is equal to the maximum throw of 30 ms). Fine, dip-parallel lines show positions of cross-sectional interpretations (spaced 12.5 m in the relay and 62.5 m outside). Footwall and hanging wall intersections with the fault surface are shown (horizon separations) for reflectors A and B. Line of section (a) indicated.

Fig. 7a and b). The fault segments link downwards along a branchline to form a continuous fault on a lower mapped horizon (Horizon B, Fig.7a and c). The relay zone and two fault segments are confined to the upper ca. 400 m of the fault, and are elements of a single more extensive fault surface that extends downwards for at least 1.5 km and laterally for at least 2 km. Displacement on Horizon B varies regularly along the fault trace shown. At higher levels displacement on the two fault segments is conserved by displacement transfer across the intervening relay zone, i.e. on any given horizon aggregate displacements on the individual segments are approximately equal to displacement immediately outwith of the relay zone. The upward decrease in displacement on the fault arises from the synsedimentary nature of the fault (i.e. it is a growth fault), with younger horizons recording less of the displacement history. Given that segmentation is limited to the upper part of the fault surface and that aggregated displacement contours are approximately parallel to the upper tip line and perpendicular to the near vertical relay zone, the formation of the relay zone is best explained by upward propagation (Fig. 7). As fault propagation was normal to the horizons and approximately vertical, the relay zone at the free surface would have been established near instantaneously on a geological timescale. Therefore, while it is tempting to interpret segments viewed on maps as having nucleated as separate, and isolated, faults, this could never have been the case in this example.

Previously published 3-D seismic and coalmine datasets (Childs et al., 1995; Huggins et al., 1995; Walsh et al., 1999), reveal that fault geometries similar to those in Fig. 7 constitute an important subset of segmented faults. Although segmented faults that join out of the plane of inspection could coincidentally form by linkage of two isolated faults, this geometry is most pragmatically interpreted as arising from bifurcation of a single fault surface.

5. Fault segmentation and bifurcation

Fault surface bifurcation, referred to as tip-line bifurcation, has been established from the analysis of 3-D fault geometries (Fig. 7; Childs et al., 1995, 1996b; Huggins et al., 1995; Walsh et al., 1999), in analogue models (Gabrielsen and Clausen, 2001) and by analogy with bifurcation during Mode 1 crack propagation documented in the material sciences literature (Kerkhof, 1973; Green et al., 1977; Hull, 1993). Tip-line bifurcation can arise from irregular tip-line propagation due to heterogeneities in the host rock material properties, such as a body or layer(s) (see Huggins et al., 1995), due to non-uniformity of stress fields (Mandl, 1987) or stress field reorientation as with reactivated faults (Woods et al., 1992). It is generally accepted that the propagation of faults is often accompanied by the formation of pre-localisation arrays of faults, referred to as process zones (Friedman et al., 1972). In 3-D these fault arrays will

form geometrically and kinematically coherent systems equivalent to that of a single isolated fault. Given that fault tip propagation involves 3-D segmentation and complex bifurcations of the parent fault surface, and the general recognition that many faults appear to be continuous on one scale but are segmented on another, we can extend the simplistic notion of a single fault surface (Fig. 5, see Section 3) to include processes that are responsible for fault segmentation. A schematic illustration of such a model is shown in Fig. 8. This type of model represents a plausible extension of the single isolated fault model, and when combined with a 3-D perspective of faults provides a basis for the coherent fault model. Figs. 1, 7 and 9 illustrate some relatively simple departures from a single propagating fault surface where the propagation direction is likely to be at an angle to, rather than within, the plane of inspection. The segmented fault arrays generated by these processes on some inspection planes may be either hard-linked or soft-linked to other fault segments or to the main fault surface. Though our schematic diagrams (Fig. 8) are for a normal fault, the same basic model could be applied to other modes of faulting (strike-slip or reverse). These diagrams illustrate only a snap-shot in time because with increasing displacement the relay zones between segments are breached and a throughgoing fault is formed (Peacock and Sanderson, 1991; Childs et al., 1995, 1996a,b; Walsh et al., 1999). The crucial aspect of this simple model is that it provides a basis for fault segmentation, which represents a significant
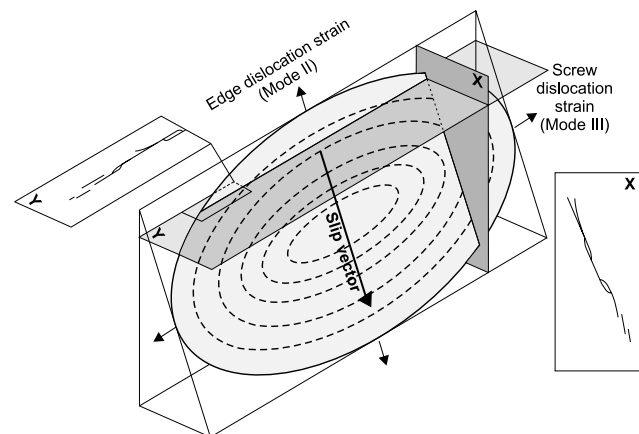

Fig. 8. (a) Schematic representation of an idealised elliptical fault (aspect ratio ca. 1.7). Maximum displacement is located in the middle of the fault and decreases systematically towards the tip-line (contours shown as dashed lines). Only the cross-section or map planes that contain the principal axes of the ellipse sample the end-member modes (II and III) of fault propagation to produce edge or screw dislocation strains. Examples of potential segmentation geometries viewed in cross-section (X) and map view (Y) are shown in the insets; the wide range of other possible segmentation geometries are not illustrated in the figure. The fault segments are small in relation to the main fault surface in this illustration but no general scale of segmentation is implied. Segmentation may occur on a wide range of scales and the main fault surface could, for example, be comprised of two unconnected segments of equal size. The beaded fault traces shown in the insets indicate fault-bounded lenses formed by the breaching of segment boundaries.
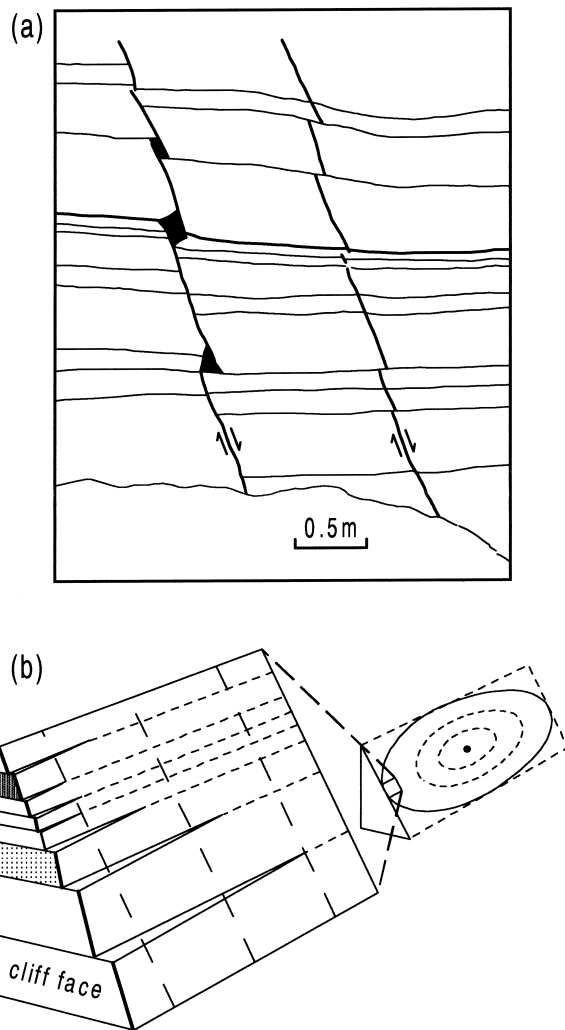
Fig. 9. (a) Vertically segmented faults viewed in a cliff face, Flamborough Head, UK (reproduced from Childs et al. 1996a). Subhorizontal lines are thin marl units or pronounced bedding surfaces between chalk units. These faults are interpreted to be close to the tips of faults with larger displacements (centimetre to metre throw) out of the plane of section as illustrated in the block diagram (b). Fault segmentation is attributed to heterogeneous propagation of the two faults in this highly anisotropic chalk-marl interbedded succession. The steep dashed lines in (b) are throw contours.
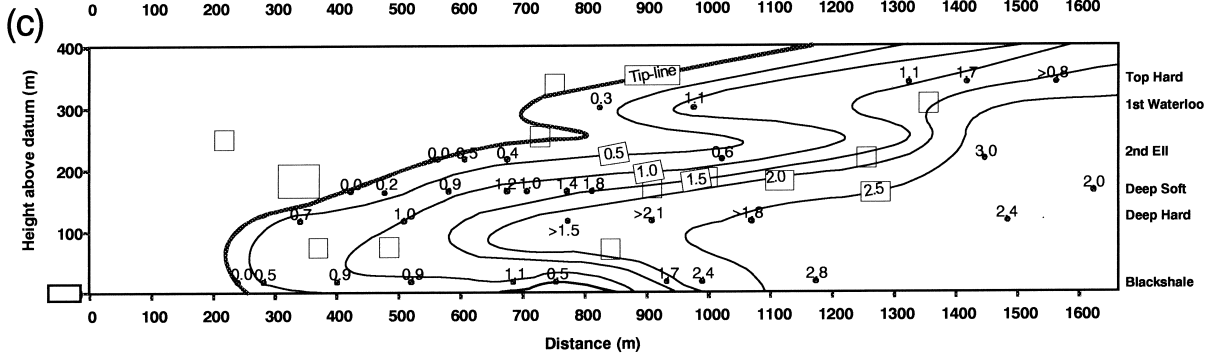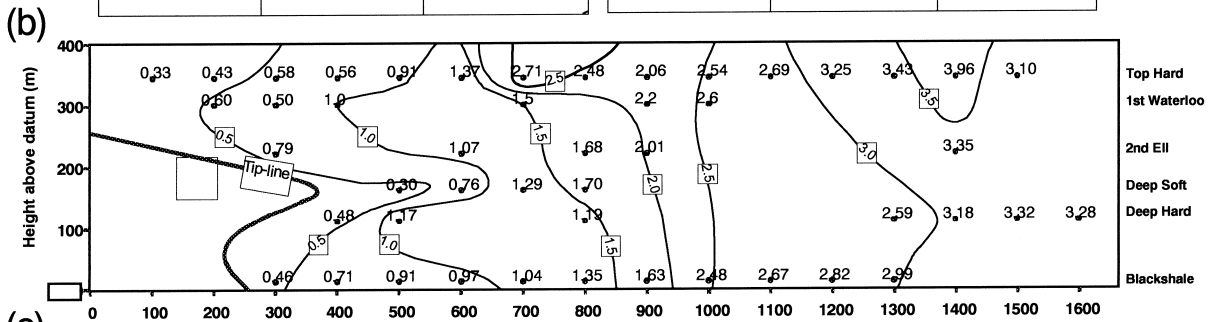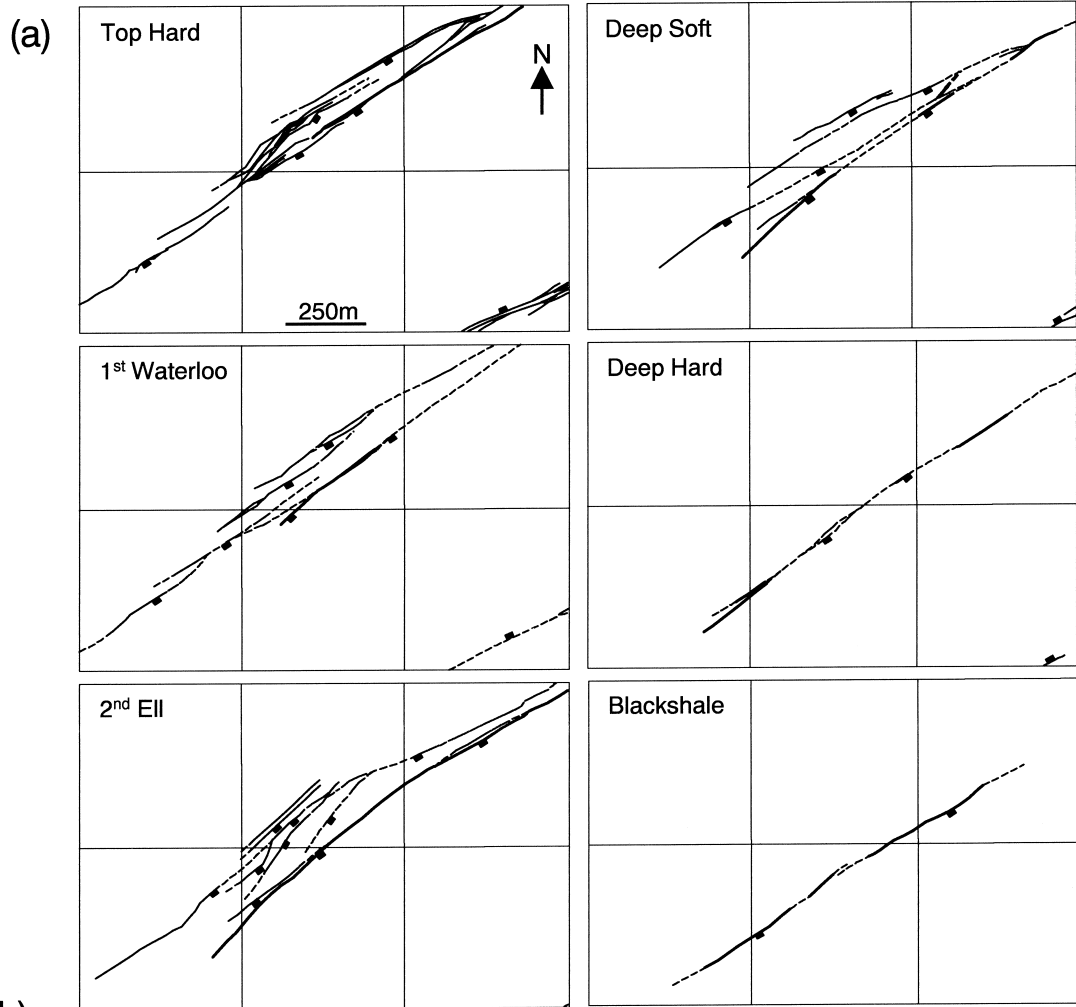
departure from models invoking the formation of segmented fault arrays by the incidental interaction of originally isolated faults i.e. the 'isolated fault' model. Incorrectly attributing segmentation formed as part of the 3-D propagation and localisation of faults, which is likely to

be most significant in layered rocks that are mechanically heterogeneous, to incidental interaction of initially isolated faults, will produce an over emphasis on the importance of linkage of isolated faults in fault growth. It is self evident that if these coherent segments are then considered in isolation they will also produce fault displacement to length ratios that are considerably greater than those for the fault as a whole (Walsh and Watterson, 1990; Gillespie et al., 1992). Therefore, failure to recognise that segments are components of a larger fault will inevitably lead to an over reliance of models on the growth of faults by linkage of isolated segments.

6. Spatial arrangement of segmented fault arrays

An additional line of evidence favouring the coherent fault model is purely geometrical. Examination of segmented fault arrays often reveals that the separation between sub-parallel fault segments occurs on a much smaller scale than that of the spacing between adjacent faults or segmented fault arrays. In Figs. 1 and 3, for example, segmented fault arrays are separated by distances that are often an order of magnitude or more greater than the separation across relay zones. An example of such a segmented fault zone mapped in three dimensions is provided by coal mine abandonment plans from Markham Colliery, Derbyshire Coalfield, UK (Fig. 10a). Successive mine plans through the fault zone demonstrate varying degrees of fault zone complexity. At the base of the succession the mapped fault zone comprises a single, approximately linear, fault trace, which widens upwards into a 200-m-wide zone comprising numerous linked and unconnected fault traces. The change in complexity of the fault zone occurs between the Deep Soft and Deep Hard seams and has been attributed to the presence of a prominent ca. 30-m-thick sandstone between these seams in the otherwise shale dominated succession (Rippon, 1985). Despite the vertical change in fault zone structure between seams, the numerous fault segments combine to define a regular aggregate displacement distribution (Fig. 10b) identifying this fault zone as a geometrically coherent unit. Although unambiguous correlation of fault traces between successive seams is not possible for each fault segment, the largest fault segment can be correlated with confidence (Fig. 10c). This segment has a reclined tip-line

Fig. 10. (a) Abandonment plans for six coal seams in an area of Markham Colliery (SK/4470), Derbyshire Coalfield, UK, centred on a NE striking fault zone; the area was initially described by Rippon (1985). All faults with throws of 6 inches (15 cm) or greater are recorded on the mine plans. The area of worked ground varies between seams, but approaches complete coverage on the Top Hard so that blank areas of the map indicate an absence of faults. Dashed fault traces are interpolated across unworked ground. (b) Aggregate throw (in metres) across the fault zone in (a). Throws on individual coal seams are summed along lines normal to the fault zone strike and are projected onto a vertical plane parallel to the fault zone, i.e. the strike projection plane. Throw sample lines are spaced every 100 m and only aggregate throws derived from lines that traverse continuous workings across the fault zone are shown. Seam elevations are shown relative to an arbitrary datum and distances are measured from the SW. Summed throws are for fault segments that dip to the SE; the total throw on NE dipping faults is everywhere less than 0.7 m. (c) Strike projection showing the throw distribution on the largest fault segment shown bold in (a). Tip-line locations in (b) and (c) are drawn through tip-points on successive coal maps but the faults are expected to extend some tens of metres beyond the mapped tip.

(a) Top Hard, Deep Soft, 1st Waterloo, Deep Hard, 2nd Ell, Blackshale

(b) Height above datum (m) vs Distance (m)

(c) Height above datum (m) vs Distance (m)

and dies out upwards over much of the mapped fault length, its displacement being transferred onto a number of smaller segments at higher levels. These smaller faults may either link to the main fault or be unconnected to the main fault, as shown by Rippon (1985). Throw contours for the fault zone as a whole are approximately vertical suggesting that the data volume lies at the lateral tip of a structure with a maximum displacement to the NE of the data area. The fault zone is separated from the nearest neighbouring fault by 750 m of unfaulted ground and it is clear that each of the component fault segments formed as part of a single structure, which probably propagated from the NE.

Similar conclusions may be drawn from the spatial relations of segmented faults at Kilve, England (Peacock, 1991), Canyonlands, USA (Cartwright et al., 1995), Flamborough Head, England (Fig. 9; Childs et al., 1996a, b) and Blackrock Quarry, South Wales (Nicol et al., 2002). In each of these examples, where the relay zone separation is small compared with fault spacings, the likelihood is low that two fault segments were positioned randomly in space. The most parsimonious explanation of the array shown in Fig. 1, for example, is that either the segments link to form a single fault surface or that they formed a coherent array from their inception. At Flamborough Head, analysis of normal faults in vertical outcrops indicates that segmented fault arrays are an order of magnitude more common than would be expected for randomly located fault segments (Childs et al., 1996a). Therefore, segmented fault arrays, which are spatially distinct from other faults, possess a degree of organisation that suggests an underlying control on fault segment locations. The simplest kinematic interpretation of these arrays is that they comprise segments produced either by bifurcation, i.e. splay formation, from a single fault surface, or by 3-D segmentation to form the en-échelon or, en-bayonet arrays, within a developing process zone (Marchal et al., 1998). Both of these processes favour the formation of segmented arrays in conjunction with 3-D propagation, rather than by exclusively within-plane propagation and incidental overlap of originally isolated and randomly located faults.

7. Discussion and conclusions

Segmented fault arrays may form by the incidental overlap of previously unrelated faults or within a kinematically coherent system as by-products of the localisation and 3-D propagation of individual faults within heterogenous rock volumes. The distinction between these two models is crucial as acceptance of one model over the other has a significant impact on our perception of fault growth. Models for the growth of segmented arrays that assume fault propagation within the plane of inspection also implicitly assume that fault growth approximates to a 2-D process and inevitably lead to the construction of 'isolated fault' models, involving the incidental overlap of previously unrelated

faults. This in turn leads to a strong bias towards fault growth by linkage of independent faults. Acknowledging that fault propagation occurs in 3-D, by contrast, provides the basis for adopting a 'coherent fault model' in which kinematically related segments arise from the propagation of individual faults through a rock volume. In this context, segments within a kinematically coherent array are components of the process zone or the damage zone associated with fault propagation; eventual breaching of the relays between fault segments is a natural consequence of the continued growth of the array and will ultimately lead to the development of an array which is hard-linked in 3-D (Fig. 8).

The best means of distinguishing between the 'isolated fault' and 'coherent fault' models using geological data are kinematic constraints on fault growth. These constraints are best derived for synsedimentary faults in areas where sedimentation rates exceed fault displacement rates. In such circumstances, fault scarps are blanketed by sediment and the fault displacement history is preserved (Petersen et al., 1992; Childs et al., 1995; Nicol et al., 1997). Published examples where conditions apply, generally support a 'coherent fault' model (Childs et al., 1995; Walsh et al., 1999; Meyer et al., 2002) with the geologically instantaneous formation of relays between fault segments. More often, however, synsedimentary faults are characterised by relatively high fault displacement rates, with the generation of partly filled hanging wall basins and uplifted, and sometimes eroded, footwalls (e.g. Contreras et al., 2000). In these circumstances, the kinematic constraints on faulting are to some extent equivocal. Available evidence suggests that arrays of faults are often developed early in the evolution of fault systems (Childs et al., 2003; Meyer et al., 2002; Walsh et al., 2002). Early coalescence of faults resulting in sedimentation patterns similar to those of a single fault has previously been suggested (Morley, 1999; Morley and Wonganan, 2000; Walsh et al., 2002) and could be attributable to either very rapid propagation rates of isolated faults (i.e. too rapid to be accurately measured or documented with the existing data) or to a coherent fault model. A distinction between either model cannot be made in other cases because the actual fault displacement cannot be measured (e.g. Contreras et al., 2000) or because account has not explicitly been taken of the continuous displacements (i.e. rotations) often associated with segment boundaries (Young et al., 2001; McLeod et al., 2000). Continuous displacements can take the form of sub-resolution faults, which McLeod et al. (2000) suggest could be responsible for the displacement minima seen along now continuous faults containing numerous breached relays. In another study (Young et al., 2001), stratigraphic evidence from the hanging wall of a fault, believed to contain numerous breached relays, suggests the presence of ponded sediment sub-basins adjacent to some paleo-fault segments. Though an 'isolated fault' model is preferred by Young et al. (2001), the sedimentary thickness changes

could reflect the complexities of sediment dispersal patterns associated with the segmented nature of the array and the presence of relays, or could even be diagnostic of the hanging wall deformation associated with a 'coherent fault' array; the hanging wall deformation associated with either model is not yet known. Whilst an isolated fault model may apply to some or all of these systems described in recent articles (Contreras et al., 2000; McLeod et al., 2000; Young et al., 2001), a coherent fault model cannot be ruled out and may be the most parsimonious explanation. Furthermore, in circumstances where fault propagation is a geologically rapid or, given the resolution of geological data, an instantaneous process, then vestiges of isolated growth are unlikely to be preserved and the kinematics of the fault array will subscribe to that of the coherent fault model.

We have outlined a variety of means of discriminating between segmented arrays generated by two models including; analysis of 3-D propagation of an ideal elliptical fault, together with consideration of the 3-D fault geometries, the spatial organisation and the aggregate displacement patterns of segmented fault arrays. This 3-D viewpoint requires that the segments comprising fault arrays are often geometrically and kinematically related from the beginning of their evolution. Propagation of a fault through a mechanically heterogeneous multi-layer as a single discrete structure is unlikely and supports the view that many segmented fault arrays previously attributed to an 'isolated fault' model are best interpreted as the products of bifurcation and 3-D segmentation of individual propagating faults. Fault segmentation could be controlled by many factors, and the scale on which segmentation occurs is likely to be controlled to a great extent by the stratigraphic and material properties of the faulted sequence.

Although we do not contest that isolated fault growth followed by incidental linkage occurs, this model should not be universally applied to all segmented normal fault arrays. In light of 3-D data and arguments presented in this paper we believe that the coherent fault model can be the most parsimonious and, therefore, preferred interpretation.

Acknowledgements

References

Anders, M.H., Schlische, R.W., 1994. Overlapping faults, intrabasin highs and the growth of normal faults. Journal of Geology 102, 165–180.

Barnett, J.A.M., Mortimer, J., Rippon, J.H., Walsh, J.J., Watterson, J., 1987. Displacement geometry in the volume containing a single normal fault. American Association of Petroleum Geologists Bulletin 71, 925–937.

Cartwright, J.A., Trudgill, B., Mansfield, C.S., 1995. Fault growth by segment linkage: an explanation for scatter in maximum displacement and trace length data from the Canyonlands Grabens of SE Utah. Journal of Structural Geology 17, 1319–1326.

Cartwright, J.A., Mansfield, C.S., Trudgill, B., 1996. The growth of normal faults by segment linkage. In: Buchanan, P.G., Nieuwland, D.A. (Eds.), Modern Developments in Structural Interpretation, Validation and Modelling. Geology Society London Special Publication 99, pp. 163–177.

Chapman, T.J., Meneilly, A.W., 1991. The displacement patterns associated with a reverse-activated, normal growth fault. In: Roberts, A.M., Yielding, G., Freeman, B. (Eds.), The Geometry of Normal Faults. Geological Society London Special Publication 56, pp. 183–192.

Childs, C., Easton, S.J., Vendeville, B.C., Jackson, M.P.A., Lin, S.T., Walsh, J.J., Watterson, J., 1993. Kinematic analysis of faults in a physical model of growth faulting above a viscous salt analogue. Tectonophysics 228, 313–329.

Childs, C., Watterson, J., Walsh, J.J., 1995. Fault overlap zones within developing normal fault systems. Journal of the Geological Society of London 152, 535–549.

Childs, C., Nicol, A., Walsh, J.J., Watterson, J., 1996a. Growth of vertically segmented normal faults. Journal of Structural Geology 18, 1389–1397.

Childs, C., Watterson, J., Walsh, J.J., 1996b. A model for the structure and development of fault zones. Journal of the Geological Society of London 153, 337–340.

Childs, C., Nicol, A., Walsh, J.J., Watterson, J., 2003. The growth and propagation of synsedimentary faults. Journal of Structural Geology in press (PII:S0191-8141(02)00054-8).

Cloos, H., 1928. Experimente zur inneren Tektonik. Centralblatt für Mineralogie, Abt. B, 609–671.

Contreras, J., Anders, M.H., Scholz, C.H., 2000. Growth of a normal fault system: observations from the Lake Malawi basin of the east African rift. Journal of Structural Geology 22, 159–168.

Cowie, P.A., 1998. A healing–reloading feedback control on the growth rate of seismogenic faults. Journal of Structural Geology 8, 1075–1087.

Cowie, P.A., Vanneste, C., Sornette, D., 1993. Statistical physics model for the spatiotemporal evolution of faults. Journal of Geophysical Research 98, 21809–21821.

Cowie, P.A., Gupta, S., Dawers, N.H., 2000. Implications of fault array evolution for synrift depocentre development: insights from a numerical fault growth model. Basin Research 12, 241–261.

Dawers, N.H., Anders, M.H., 1995. Displacement–length scaling and fault linkage. Journal of Structural Geology 17, 607–614.

Eisenstadt, G., De Paor, D.G., 1987. Alternative model of thrust–fault propagation. Geology 15, 630–633.

Friedman, M., Handin, J., Alani, G., 1972. Fracture–surface energy of rocks. International Journal of Rock Mechanics and Mining Sciences 9, 757–766.

Gabrielsen, R.H., Clausen, J.A., 2001. Horses and duplexes in extensional regimes: a scale-modeling contribution. In: Koyi, H.A., Mancktelow, N.S. (Eds.), Tectonic Modelling: A Volume in Honour of Hans Ramberg. Geological Society of America Memoir 193, pp. 207–220.

Gillespie, P.A., Walsh, J.J., Watterson, J., 1992. Limitations of dimension and displacement data from single faults and the consequences for data analysis and interpretation. Journal of Structural Geology 14, 1157–1172.

Green, D.J., Nicholson, P.S., Embury, J.D., 1977. Crack shape studies in brittle porous materials. Journal of Materials Science 12, 987–989.

Gupta, A., Scholz, C.H., 2000. A model of normal fault interaction based on observations and theory. Journal Structural Geology 22, 865–879.

Gupta, S., Cowie, P.A., Dawers, N.H., Underhill, J.R., 1998. A mechanism to explain syn-rift basin subsidence and stratigraphic patterns through fault array evolution. Geology 26, 595–598.

Huggins, P., Watterson, J., Walsh, J.J., Childs, C., 1995. Relay zone

geometry and displacement transfer between normal faults recorded in coal-mine plans. Journal of Structural Geology 17, 1741–1755.

Hull, D., 1993. Tilting cracks: the evolution of fracture surface topography in brittle solids. International Journal of Fractures 62, 119–138.

Kerkhof, F., 1973. Wave fractographic investigations of brittle fracture dynamics. In: Sih, G.C., (Ed.), Proceedings of an International Conference on Dynamic Crack Propagation, Noordhof International Publishing, pp. 3–35.

Mandl, G., 1987. Discontinuous fault zones. Journal of Structural Geology 9, 105–110.

Mansfield, C., Cartwright, J.A., 1998. High resolution fault displacement mapping from three-dimensional seismic data: evidence for dip linkage during fault growth. Journal of Structural Geology 18, 249–263.

Mansfield, C., Cartwright, J.A., 2001. Fault growth by linkage: observations and implications from analogue models. Journal of Structural Geology 23, 745–763.

Marchal, D., Guiraud, M., Rives, T., Van Den Driessche, J., 1998. Space and time propagation processes of normal faults. In: Jones, G., Fisher, Q.J., Knipe, R.J. (Eds.), Faulting, Fault Sealing and Fluid Flow in Hydrocarbon Reservoirs. Geological Society London Special Publication 147, pp. 51–70.

McLeod, A.E., Dawers, N.H., Underhill, J.R., 2000. The propagation and linkage of normal faults: insights from the Strathspey–Brent–Statfjord fault array, northern North Sea. Basin Research 12, 263–284.

Meyer, V., Nicol, A., Childs, C., Walsh, J.J., Watterson, J., 2002. Progressive localisation of strain during the evolution of a normal fault system in the Timor Sea. Journal of Structural Geology 24, 1215–1231.

Morley, C.K., 1999. Patterns of displacement along large normal faults: implications for basin evolution and fault propagation, based on examples from East Africa. Bulletin of the American Association of Petroleum Geologists 83, 613–634.

Morley, C.K., Wonganan, N., 2000. Normal fault displacement characteristics, with particular reference to synthetic transfer zones, Mae Moh mine, northern Thailand. Basin Research 12, 307–327.

Morley, C.K., Nelson, R.A., Patton, T.L., Munn, S.G., 1990. Transfer zones in the East African rift system and their relevance to hydrocarbon exploration in rifts. American Association of Petroleum Geologists Bulletin 74, 1234–1253.

Nicol, A., Watterson, J., Walsh, J.J., Childs, C., 1996. The shapes, major axis orientations and displacement patterns of fault surfaces. Journal of Structural Geology 18, 235–248.

Nicol, A., Walsh, J.J., Watterson, J., Underhill, J.R., 1997. Displacement rates of normal faults. Nature 390, 157–159.

Nicol, A., Gillespie, P.A., Childs, C., Walsh, J.J., 2002. Relay zones between mesoscopic thrust faults in layered sedimentary sequences. Journal of Structural Geology 24, 709–727.

Peacock, D.C.P., 1991. Displacements and segment linkage in strike-slip fault zones. Journal of Structural Geology 13, 1025–1035.

Peacock, D.C.P., Sanderson, D.J., 1991. Displacements, segment linkage and relay ramps in normal fault zones. Journal of Structural Geology 13, 721–733.

Peacock, D.C.P., Sanderson, D.J., 1994. Geometry and development of relay ramps in normal fault systems. American Association of Petroleum Geologists Bulletin 78, 147–165.

Petersen, K., Clausen, O.R., Korstgård, J.A., 1992. Evolution of a salt-related listric growth fault near the D-1 well, block 5605, Danish North Sea: displacement history and salt kinematics. Journal of Structural Geology 14, 565–577.

Richard, P.D., Naylor, M.A., Koopman, A., 1995. Experimental models of strike-slip tectonics. Petroleum Geoscience 1, 71–80.

Riedel, W., 1929. Zur Mechanik geologischer Brucherscheingen. Zentralblatt für Mineralogie, Geologie und Palaeontologie, Abhandlung B, 354–368.

Rippon, J.H., 1985. Contoured patterns of throw and hade of normal faults in Coal Measures (Westphalian) of north-east Derbyshire. Proceedings of the Yorkshire Geological Society 45, 127–161.

Stewart, I.S., Hancock, P.L., 1991. Scales of structural heterogeneity with neotectonic normal fault zones in the Aegean region. Journal of Structural Geology 13, 191–204.

Tchalenko, J.S., 1970. Similarities between shear zones of different magnitudes. Bulletin of the Geological Society of America 81, 1625–1640.

Trudgill, B., Cartwright, J., 1994. Relay-ramp forms and normal fault linkages, Canyonlands National Park, Utah. Bulletin of the Geological Society of America 106, 1143–1157.

Walsh, J.J., Watterson, J., 1987. Distributions of cumulative displacement and seismic slip on a single normal fault surface. Journal of Structural Geology 9, 1039–1046.

Walsh, J.J., Watterson, J., 1989. Displacement gradients on fault surfaces. Journal of Structural Geology 11, 307–316.

Walsh, J.J., Watterson, J., 1990. New methods of fault projection for coalmine planning. Proceedings of the Yorkshire Geological Society 48, 209–219.

Walsh, J.J., Watterson, J., 1991. Geometric and kinematic coherence and scale effects in normal fault systems. In: Roberts, A.M., Yielding, G., Freeman, B. (Eds.), The Geometry of Normal Faults. Geological Society London Special Publication 56, pp. 193–203.

Walsh, J.J., Watterson, J., Childs, C., Nicol, A., 1996. Ductile strain effects in the analysis of seismic interpretations of normal fault systems. In: Buchanan, P.G., Nieuwland, D.A. (Eds.), Modern Developments in Structural Interpretation, Validation and Modelling. Geological Society London Special Publication 99, pp. 27–40.

Walsh, J.J., Watterson, J., Bailey, W., Childs, C., 1999. Fault relays, bends and branch-lines. Journal of Structural Geology 21, 1019–1026.

Walsh, J.J., Nicol, A., Childs, C., 2002. An alternative model for the growth of faults. Journal of Structural Geology 24, 1669–1675.

Watterson, J., 1986. Fault dimensions, displacements and growth. Pure and Applied Geophysics 124, 365–373.

Willemse, E.J.M., 1997. Segmented normal faults: correspondence between three-dimensional mechanical models and field data. Journal of Geophysical Research 102, 675–692.

Willemse, E.J.M., Pollard, D.D., Aydin, A., 1996. Three-dimensional analyses of slip distributions on normal fault arrays with consequences for fault scaling. Journal of Structural Geology 18, 295–309.

Woods, E.P., 1992. Vulcan sub-basin fault styles—implications for hydrocarbon migration and entrapment. Australian Petroleum Exploration Association Journal 32, 138–158.

Young, M.J., Gawthorpe, R.L., Hardy, S., 2001. Growth and linkage of a segmented normal fault zone; the Late Jurassic Murchison–Statfjord Fault, northern North Sea. Journal of Structural Geology 23, 1933–1952.